Expression of the oncofetal ED-B–containing fibronectin isoform in hematologic tumors enables ED-B–targeted ^{131}I-L19SIP radioimmunotherapy in Hodgkin lymphoma patients

*Stefanie Sauer,[1] *Paola A. Erba,[2] Mario Petrini,[3] Andreas Menrad,[4] Leonardo Giovannoni,[5] Chiara Grana,[6] Burkhard Hirsch,[1] Luciano Zardi,[7] Giovanni Paganelli,[6] Giuliano Mariani,[2] Dario Neri,[8] †Horst Dürkop,[1] and †Hans D. Menssen[9]

[1]Department of Pathology, Campus Benjamin Franklin, Charité-Universitätsmedizin, Berlin, Germany; [2]Regional Center of Nuclear Medicine and [3]Department of Hematology, University of Pisa Medical School, Pisa, Italy; [4]Genzyme Europe Research, Cambridge Science Park, Cambridge, United Kingdom; [5]Philogen SpA, Siena, Italy; [6]Department of Nuclear Medicine, European Institute of Oncology, Milan, Italy; [7]Laboratory of Innovative Therapies, Centro Biotecnologie Avanzate, Genova, Italy; [8]Department of Chemistry and Applied Biosciences, Institute of Pharmaceutical Sciences, Swiss Federal Institute of Technology (ETH), Zurich, Switzerland; and [9]Department of Global Clinical Development Oncology, Bayer HealthCare Pharmaceuticals, Montville, NJ

Current treatment of hematologic malignancies involves rather unspecific chemotherapy, frequently resulting in severe adverse events. Thus, modern clinical research focuses on compounds able to discriminate malignant from normal tissues. Being expressed in newly formed blood vessels of solid cancers but not in normal mature tissues, the extradomain B of fibronectin (ED-B FN) is a promising target for selective cancer therapies. Using immunohistology with a new epitope retrieval technique for paraffin-embedded tissues, ED-B FN expression was found in biopsies from more than 200 Hodgkin and non-Hodgkin lymphoma patients of nearly all entities, and in patients with myeloproliferative diseases. ED-B FN expression was nearly absent in normal lymph nodes (n = 10) and bone marrow biopsies (n = 9). The extent of vascular ED-B FN expression in lymphoma tissues was positively correlated with grade of malignancy. ED-B FN expression was enhanced in lymph nodes with severe lymphadenopathy and in some hyperplastic tonsils. The in vivo accessibility of ED-B FN was confirmed in 3 lymphoma patients, in whom the lymphoma lesions were visualized on scintigraphy with ^{131}I-labeled L19 small immunoprotein (^{131}I-L19SIP). In 2 relapsed Hodgkin lymphoma patients, ^{131}I-L19SIP radioimmunotherapy induced a sustained partial response, qualifying ED-B FN as a promising target for antibody-based lymphoma therapies. (Blood. 2009;113:2265-2274)

Introduction

Most anticancer therapies cannot discriminate between malignant and normal tissues, since their action depends on the increased proliferation rate of tumor versus benign cells.[1] Furthermore, high systemic doses of cytotoxic/cytostatic drugs are generally required to achieve therapeutically active concentrations within the tumor, thus frequently resulting in severe adverse effects. The approach of antibody-based therapies to selectively target therapeutically active molecules to tumor tissues is highly promising. Few of such immunotherapy agents are currently in clinical development or have been approved for treating solid cancers or hematologic malignancies (Mylotarg, EMD273063).[2,3] The basic prerequisite to apply this strategy is tumor-selective expression of the specific target structure. The extradomain B of fibronectin (ED-B FN) has been suggested as a potential target for novel anticancer therapies in patients with solid tumors.[4]

Fibronectin (FN) is a ubiquitously expressed high-molecular-weight extracellular matrix glycoprotein that exists in various isoforms.[5,6] Sequence analysis has revealed that FN consists of 3 different sequence homologies designated as type I, II, and III repeats.[7] Three sites of alternative splicing within the type III repeats of the FN molecule have so far been identified: ED-A (type III homology extradomain A), ED-B (type III homology extradomain B), and IIICS (type III homology connecting segment).[8]

Since the ED-B domain is preferentially expressed by transformed cells in vitro,[9] ED-B FN was designated as oncofetal or embryonic FN, reflecting its expression mainly in fetal tissues and solid tumors.[10,11] ED-B FN is synthesized, secreted, and deposited to the extracellular matrix structures by numerous cell types such as endothelial cells of newly formed blood vessels, myofibroblasts, and, most notably, tumor cells.[12-15] It can be detected at the abluminal site of endothelial linings of newly formed blood vessels and between stromal structures. Using polyclonal, monoclonal, and recombinant antibodies for antigen detection by immunohistochemistry (IH), ED-B FN expression can be demonstrated in a variety of human tissues.[10,16-18] ED-B FN expression is tightly controlled and appears to be restricted to embryonic tissues, a few normal adult organs, and wound healing.[10,11,19] However, the functional significance of ED-B-FN is still to be established. In vitro studies have yielded contradictory results, and studies with in vivo models on single deletion of EIIIA or EIIIB have failed to provide significant insight into the possible functions of these splice variants. In fact, EIIIA-null or EIIIB-null mice are viable, are fertile, and maintain normal physiological angiogenesis after birth.[20,21] Nevertheless, EIIIA/

Submitted May 30, 2008; accepted December 11, 2008. Prepublished online as *Blood* First Edition paper, January 8, 2009; DOI 10.1182/blood-2008-06-160416.

*S.S. and P.A.E. contributed equally to the study.

†H.D. and H.D.M. contributed equally to the study.

An Inside *Blood* analysis of this article appears at the front of this issue.

The publication costs of this article were defrayed in part by page charge payment. Therefore, and solely to indicate this fact, this article is hereby marked "advertisement" in accordance with 18 USC section 1734.

Table 1. ED-B FN expression in hematopoietic malignancies

Entity	Percentage ED-B FN+ vessels			
	More than 90%	50%-90%	10%-50%	Less than 10%
Low malignant B-NHL				
Plasmacytoma	6/14	6/14	2/14	0/14
Mantle cell lymphoma	6/12	3/12	2/12	1/12
Lymphocytic lymphoma (CLL)	3/11	2/11	4/11	2/11
Marginal zone lymphoma	2/4	2/4	0/4	0/4
Lymphoplasmocytic lymphoma	2/3	0/3	1/3	0/3
Follicular lymphoma (FL)				
FL grade 1	2/5	2/5	1/5	0/5
FL grade 2	6/19	10/19	2/19	1/19
High malignant B-NHL				
FL grade 3	6/6	0/6	0/6	0/6
Diffuse large B-cell lymphoma (DLBCL)	26/38	6/38	3/38	3/38
Centroblastic	19/22	3/22	0/22	0/22
Centroimmunoblastic	4/5	1/5	0/5	0/5
Anaplastic	2/4	2/4	0/4	0/4
Immunoblastic	1/1	0/1	0/1	0/1
Plasmoblastic	0/3	0/3	2/3	1/3
T-cell rich	0/3	0/3	1/3	2/3
B-lymphoblastic lymphoma	0/4	3/4	1/4	0/4
T-NHL				
Anaplastic large T-cell lymphoma	7/14	1/14	4/14	2/14
T lymphoblastic lymphoma	4/7	2/7	1/7	0/7
Peripheral T-NHL (NOS)	4/5	0/5	1/5	0/5
Hodgkin lymphoma				
Classical Hodgkin lymphoma (cHL)	28/50	13/50	6/50	3/50
Mixed cellularity	12/24	4/24	6/24	2/24
Nodular sclerosis	16/23	6/23	0/23	1/23
Lymphocyte rich	0/3	3/3	0/3	0/3
Lymphocyte-predominant HL	3/7	3/7	0/7	1/7
Chronic myeloproliferative disease				
Chronic myelogenous leukemia	0/5	1/5	2/5	2/5
Chronic idiopathic myelofibrosis	2/4	1/4	1/4	0/4
Essential thrombocythemia	0/4	0/4	2/4	2/4
Polycythemia vera	0/4	0/4	2/4	2/4
Acute myeloblastic leukemia	0/7	3/7	4/7	0/7

Semiquantitative analysis of ED-B FN expression in lymphoid and hematopoietic tumors.

EIIIB double-null embryos display multiple cardiovascular defects, thus indicating a crucial involvement in angiogenesis and in cardiovascular development of the EIIIA- and EIIIB-containing splice variants of FN.[22]

Although physiologic expression of ED-B FN is rare in healthy adults, it can occur in chronic pathological conditions associated with new blood vessel formation[23,24] such as ocular-retinal diseases,[25,26] severe atherosclerosis,[27] and inflammatory rheumatoid disease.[28] ED-B FN is abundant in tissues of almost all human solid cancers, irrespective of histotype.[4]

Since ED-B FN expression has been more extensively evaluated in solid cancers, we thought it worthwhile to explore this biologic event also in a broad range of hematologic malignancies and normal lymphoid and hematopoietic tissues. Moreover, in vivo targeting of ED-B FN was evaluated in 3 lymphoma patients using a radiolabeled ED-B FN binding antibody (^{131}I-L19SIP), as was the clinical response in these patients to a subsequent therapeutic dose of ^{131}I-L19SIP.

Methods

Specimens

Paraffin-embedded and shock-frozen specimen of hematopoietic malignancies were drawn from the files of the Institute of Pathology, Campus Benjamin Franklin, Charité, Berlin, Germany (Table 1). In addition, 3 lymph node biopsies with the diagnosis of Epstein-Barr virus (EBV)–associated lymphoproliferation, 13 tonsils with follicular hyperplasia, 10 tumor-free lymph nodes harvested from the drainage of carcinomas, 12 enlarged lymph nodes with severe inflammation, and 9 bone marrow biopsies with nonneoplastic alterations were included in the study (Table 2). Finally, frozen specimens of 2 CLL, 6 mantle cell, and 3 follicular lymphomas were analyzed. The hematopoietic tumors were classified according to WHO classification.[29] Paraffin-embedded and frozen specimens of 6 cases of clear cell renal cell carcinoma were included as positive controls.

The mouse embryonal teratocarcinoma cell line F9 was purchased from ATCC (Manassas, VA). Athymic nude mice (8-week-old nude/nude CD1 mice, females) were obtained from Harlan, Italy (Correzzana, Milan, Italy). Nude mice were subcutaneously implanted with F9 cells as described.[30] F9 tumors, known for their strong ED-B FN expression, were harvested when approximately 10 mm in diameter and split in half. One-half was paraffin-embedded, whereas the other half was shock-frozen in liquid nitrogen. All animal experiments were conducted in accordance with the United Kingdom Coordinating Committee on Cancer Research (UKCCCR) regulations for the welfare of animals and the German animal protection law. In addition, approval was granted by local authorities from the government of Berlin LaGeSo.

Immunohistochemistry

To retrieve the ED-B FN epitope, paraffin-embedded specimens were pretreated by steam pressure boiling in 2 mM EDTA, pH 8.0, for 5 minutes.

Table 2. ED-B FN expression on blood vessels in normal lymphatic tissues and lymphatic tissues altered by nonneoplastic disease

Entity	Perivascular ED-B FN expression, percentage EB-D$^+$ vessels			
	More than 90%	50%-90%	10%-50%	Less than 10%
Normal lymphoid and hematopoietic tissues				
Normal lymph nodes	0/10	0/10	1/10	9/10
Normal bone marrow biopsies	0/9	0/9	0/9	9/9
Hyperplastic lymphoid tissues				
Hyperplastic lymph nodes	5/12	6/12	0/12	1/12
Hyperplastic tonsils	7/13	0/13	1/13	5/13

Semiquantitative analysis of ED-B FN expression in normal and inflammatory altered lymphoid tissues. The extent of ED-B expression was classified according to the indicated percentages of ED-B FN–positive vessels.

Immunohistochemistry of cryostat sections and pretreated paraffin sections was performed using the alkaline phosphatase anti-alkaline phosphatase (APAAP) method.[31] ED-B FN was detected using the dimeric L19IL2 fusion protein, which consists of the human anti–ED-B scFv L19 fused to IL-2[32,33] and MX1, an ED-B–specific murine IgG2a monoclonal antibody binding to a different epitope than L19 (A.M., February 2005, unpublished results). In each case, 10 microscopic fields were examined for ED-B FN expression in blood vessels and stroma at ×400 magnification. ED-B FN expression was semiquantitatively scored by assigning all cases to 4 categories based on the fraction of ED-B FN–positive blood vessels (ie, > 90%, between 50% and 90%, between 10% and 49%, or < 10%). These scores were applied by 2 different investigators (S.S., H.D.), reaching best interobserver agreement. Light microscopy was performed using an Olympus AX70 microscope (Tokyo, Japan) equipped with a zoom ocular and the following PlanAPO objectives: 2×/0.08, 4×/0.16, 10×/0.40, 20×/0.7, and 40×/0.95.

For ED-B FN/CD34 double fluorescence staining, ED-B FN was detected by MX1 and goat anti–mouse Cy3-conjugated antisera (Dianova, Hamburg, Germany), using a confocal microscope (Leitz, Wetzlar, Germany). After blocking the murine immunoglobulins with an excess of goat anti–mouse serum, CD34 (QBEND; Immunotech, Marseille, France) was stained and subsequently detected by goat anti–mouse Cy2-conjugated antisera (Dianova). Nuclei were depicted by TOTO-3 (Molecular Probes, Paisley, United Kingdom).

Competition experiments were performed by titrating recombinant ED-B FN against MX1 mAb and L19IL2 constructs. Subsequently, the ED-B FN immunohistologic staining properties of these mixtures were tested.

^{131}I-L19SIP SPECT-CT images and ^{18}F-FDG PET scans

Within the framework of a Health Care Authority–approved clinical trial sponsored by Philogen SpA, the pharmacokinetic profile, the dosimetry estimates, and the safety of ^{131}I-L19SIP are being investigated in lymphoma patients at the Regional Center of Nuclear Medicine, University of Pisa Medical School and at the European Institute of Oncology (IEO). Institutional board approval was obtained from all participating institutions (University of Pisa, Pisa, Italy; European Institute of Oncology, Milan, Italy) for these studies and patient informed consent was obtained in accordance with the Declaration of Helsinki. According to this study, ^{131}I-L19SIP was intravenously injected in a 73-year-old male patient with advanced relapsed small lymphocytic non-Hodgkin lymphoma (SLL NHL; NHL1), a 28-year-old male (HL1), and a 27-year-old female patient (HL2) with classical Hodgkin lymphoma of nodular sclerosis (HL). These patients had failed multiple chemotherapies, chemoradiotherapies, and immunotherapies and presented with relapsed disease as documented by computed tomography (CT) and ^{18}F-fluorodeoxyglucose positron emission tomography CT (^{18}F-FDG PET-CT) scans. ^{131}I-L19SIP (5 mCi [185 MBq]) was first administered for biodistribution and dosimetry evaluations. Whole-body scans and single photon emission computed tomography (SPECT) images (GE Infinia Hawkeye; GE Healthcare, Little Chalfont, United Kingdom) were acquired at different time points after ^{131}I-L19SIP injection, as described.[34] In particular, SPECT-CT images were acquired 48 hours, 96 hours, and 8 days after injection. Blood effective half-lives ($T_{1/2}\alpha$ and $T_{1/2}\beta$) were calculated and dosimetry to normal organs and to lesions was estimated as absorbed dose (Gy). Based on selective uptake into tumor lesions and on adequate bone marrow dosimetry (lesion/red marrow absorbed dose ratio ≥ 10), patients NHL1 and HL1 subsequently received a dose of ^{131}I-L19SIP of 5.55 GBq (150 mCi), whereas patient HL2 received a ^{131}I-L19SIP dose of 3.7 GBq (100 mCi). Whole-body and SPECT-CT images were obtained 8 to 12 days after administration of this dose to confirm specific tumor targeting.

Statistical analyses

Statistical analyses were performed with the U/H-ranking tests using 13.0 Base System SPSS for Windows (SPSS Software, Munich, Germany).

Results

Reliability and localization of ED-B FN detection in paraffin-embedded specimens

This study presents the first systematic data about the detection of the ED-B epitope of FN in paraffin-embedded tissues. To verify the expression pattern of ED-B FN in paraffin-embedded tissues, we used the mAb MX1 and the fusion protein L19IL2. Both anti–ED-B FN constructs detected the same ED-B FN expression pattern in paraffin-embedded and frozen specimens of renal carcinoma (n = 6), lymphocytic lymphoma (CLL; n = 2), mantle cell lymphoma (n = 6), and follicular lymphoma (n = 3). Identical ED-B FN expression patterns were also found in the paraffin-embedded half and the frozen half of the split F9 tumor specimens (Figure 1).

To confirm the binding specificity of the MX1 mAb and the L19IL2 fusion protein, these reagents were preincubated with an excess of recombinant ED-B FN. The mixtures were incubated on human clear cell renal cell carcinomas and murine F9 teratocarcinoma with subsequent immunohistologic detection of their binding pattern. Recombinant ED-B FN was capable of inhibiting the immunohistologic binding of these reagents (Figure 2).

Double stainings of diffuse large B-cell lymphoma, marginal zone lymphoma, lymphocytic lymphoma, plasmacytoma, follicular lymphoma (grades 1 and 3), and classic Hodgkin lymphoma (mixed cellularity and nodular sclerosis) revealed that ED-B FN is mostly colocalized with blood vessels, which were identified by their CD34$^+$ endothelia (Figure 3). By investigating 1 normal lymph node, 1 lymph node with lymphadenopathy, 1 hyperplastic tonsil, and 2 normal bone marrow samples, we also confirmed that the mostly small ED-B FN deposits are localized perivascular in nonmalignant lymphoid and hematopoietic tissues.

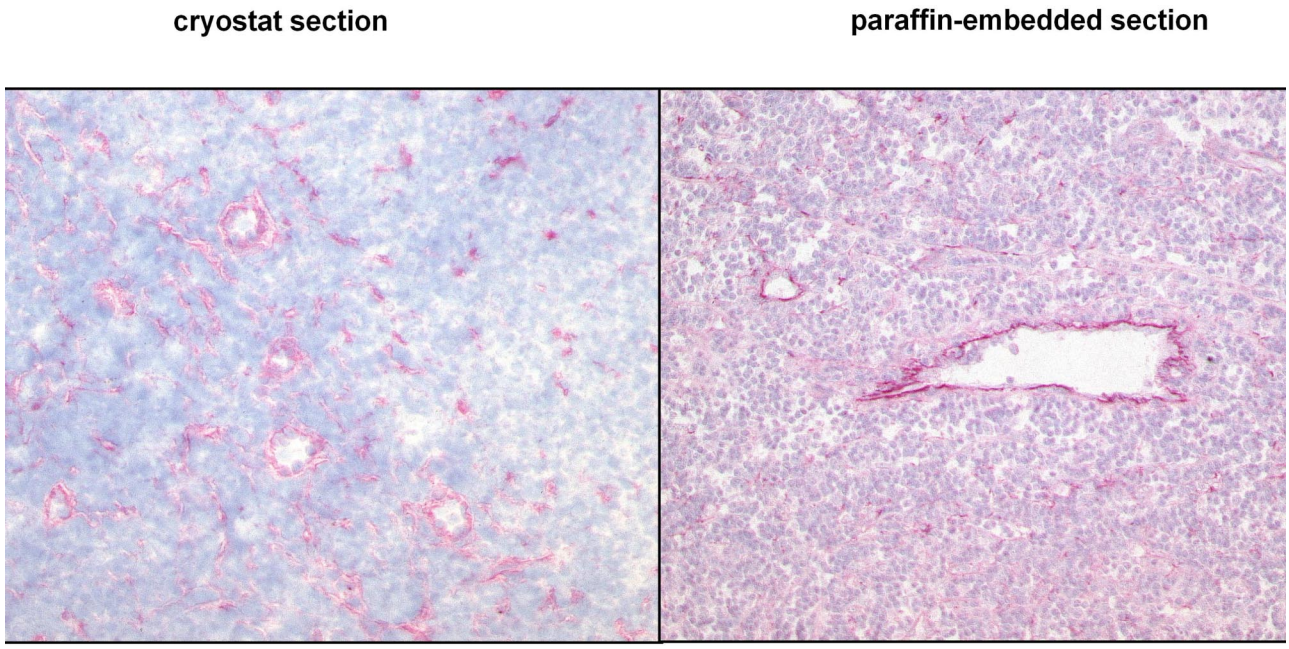

Figure 1. ED-B FN expression is similarly detectable in cryostat and paraffin-embedded tissues by immunohistology. Cryostat and paraffin-embedded specimens stemmed from the same lymph node biopsy of a patient with follicular lymphoma grade 2. One-half of the biopsy was shock-frozen, whereas the other half was paraffin-embedded. Both specimens were stained with the anti–ED-B FN MX1 antibody (magnification of the left panel: ×30; magnification of the right panel: ×50).

ED-B FN expression in normal and hyperplastic lymphoid tissue and normal bone marrow

Blood vessels of normal lymphoid tissue rarely and weakly express ED-B FN (Figure 4). ED-B FN expression in hyperplastic tonsils was heterogeneous. More than 90% of all blood vessels were ED-B FN positive in 7 of 13 tonsils, whereas 5 of 13 tonsils show very low perivascular ED-B FN expression (Table 2). Most of the ED-B FN–positive blood vessels of hyperplastic tonsils were found at the rim of germinal centers inside the inner mantle and marginal zone surrounding the highly proliferating follicular center cells. A few ED-B FN–positive vessels were situated in the fibrous fascicles of tonsils formed during chronic inflammation. ED-B FN expression was found in blood vessels of every diameter in lymphoid tissues.

Normal bone marrow samples revealed ED-B FN expression in less than 10% of all medium-sized and large blood vessels. The few ED-B FN–positive medullar vessels bore a fibrous wall. ED-B FN expression was not found in normal sinusoids lacking fibrous support.

ED-B FN expression in nodal and extranodal lymphomas

Nodal and extranodal lymphomas showed significantly more ED-B FN–positive blood vessels than normal lymphoid tissues ($P < .001$; Table 1). This finding was true for both non-Hodgkin and Hodgkin lymphomas. The degree of ED-B FN expression did not depend on the infiltrated organ, as lymphoma infiltration increased ED-B expression to almost the same extent in both nodal and parenchymal sites. High-grade malignant lymphomas (DLBCL, follicular lymphoma grade 3, and ALL) exhibited significantly higher expression of ED-B FN in blood vessels than small B-cell lymphomas (follicular lymphoma grades 1 and 2, CLL, mantle cell

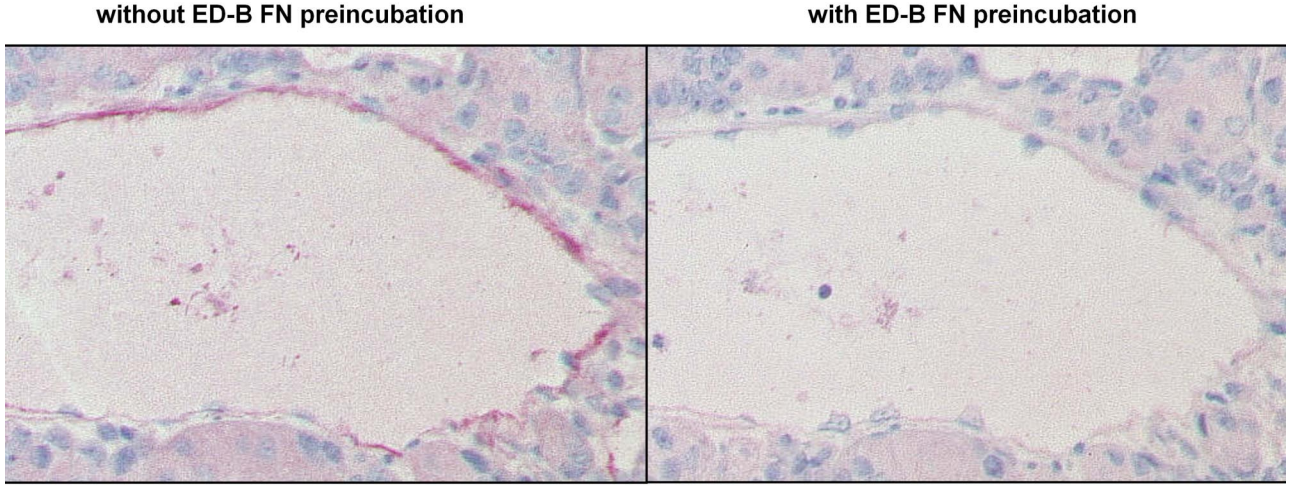

Figure 2. Competition of ED-B FN staining by soluble recombinant ED-B FN. ED-B FN immunostaining was performed on paraffin-embedded serial sections of a clear cell renal cell carcinoma, using L19IL2, with (right) or without (left, positive control) preincubation of L19IL2 with an excess of soluble recombinant ED-B (magnification: ×150).

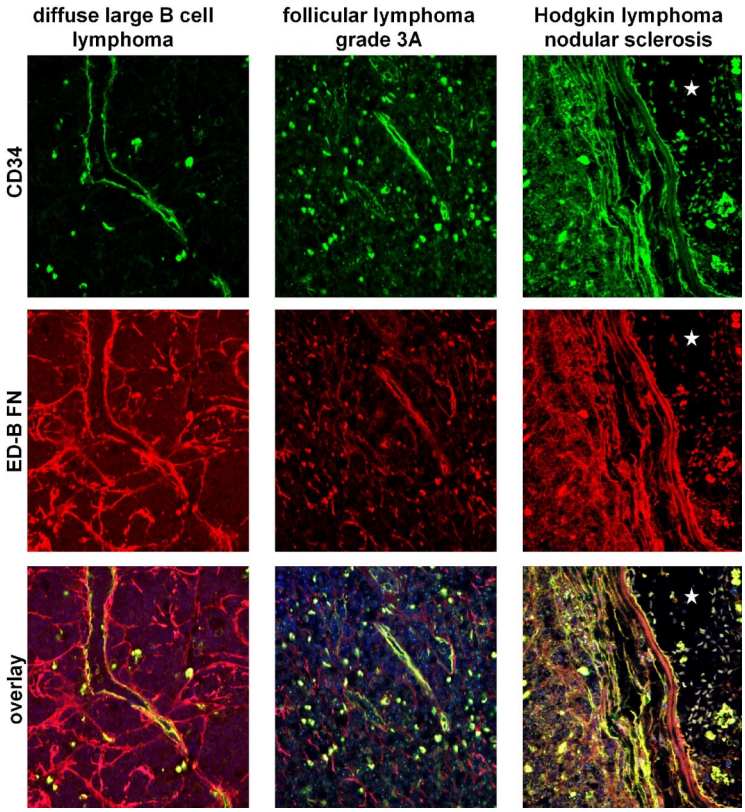

Figure 3. Double fluorescence staining of CD34⁺ endothelia (green label) and ED-B FN (red label) indicates colocalization of both antigens. The colocalization of CD34⁺ endothelia and ED-B FN was investigated by double fluorescence confocal microscopy of paraffin-embedded specimens of diffuse large B-cell lymphoma, follicular lymphoma (Grad 3a), and classic Hodgkin lymphoma. Colocalization of ED-B FN and CD34⁺ endothelia was found as indicated by the yellow label. Nuclei were stained blue (TOTO3). The asterisks in the right panels (classic Hodgkin lymphoma) indicate a large vessel lumen.

lymphoma, marginal cell lymphoma, plasmacytoma, and lymphoplasmocytic lymphoma; $P = .008$). ED-B FN expression was found in blood vessels of all diameters and locations. Vessels inside the tumor, in the tumor stroma, and the tumor capsule bear ED-B FN, whereas ED-B FN expression was not detectable in vessels at the rim of tumor necrosis. ED-B FN expression did not significantly differ between classical Hodgkin lymphoma and lymphocytic-predominant Hodgkin lymphoma.

Three cases of EBV-associated lymphoproliferation (resembling diffuse large B-cell lymphoma) showed high perivascular ED-B FN expression roughly to the same amount as in high-grade malignant lymphoma.

However, lymphoid tissue with severe inflammation, such as lymph nodes with lymphadenopathy or hyperplastic tonsils causing angina, revealed perivascular ED-B FN expression to almost the same extent as in malignant lymphoma.

ED-B FN expression in neoplastic infiltrates of the bone marrow

In comparison with normal bone marrow, ED-B FN expression was enhanced in the bone marrow inflicted by myeloproliferative disease ($P < .001$). The amount of ED-B FN–positive blood vessels did not significantly differ between acute myeloblastic

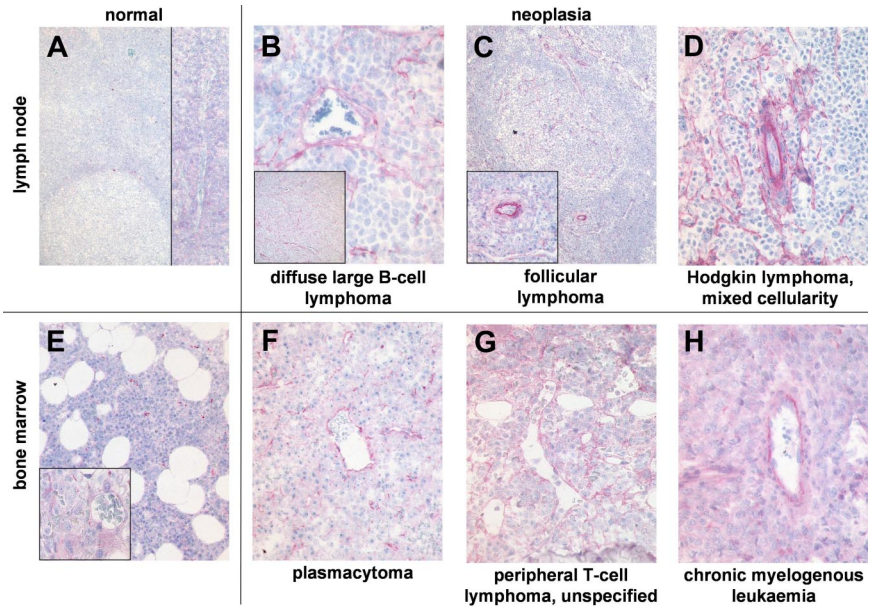

Figure 4. ED-B FN expression is abundant in biopsies of hematologic malignancies. ED-B FN expression of paraffin-embedded specimens of normal lymph node (A; magnification: ×100, left inset: ×20), and lymph node biopsies of diffuse large B-cell lymphoma (B; ×250, inset ×20); follicular lymphoma grade 2 (C; ×20, inset ×100), and classic Hodgkin lymphoma of mixed cellularity subtype (D; ×150). ED-B FN expression of bone marrow biopsies of normal bone marrow (E; ×50, inset ×200), multiple myeloma (F; ×100), unspecified peripheral T-cell lymphoma (G; ×200), and chronic myelogenous leukemia (H; ×200). All ED-B FN stainings were performed with the MX1 antibody.

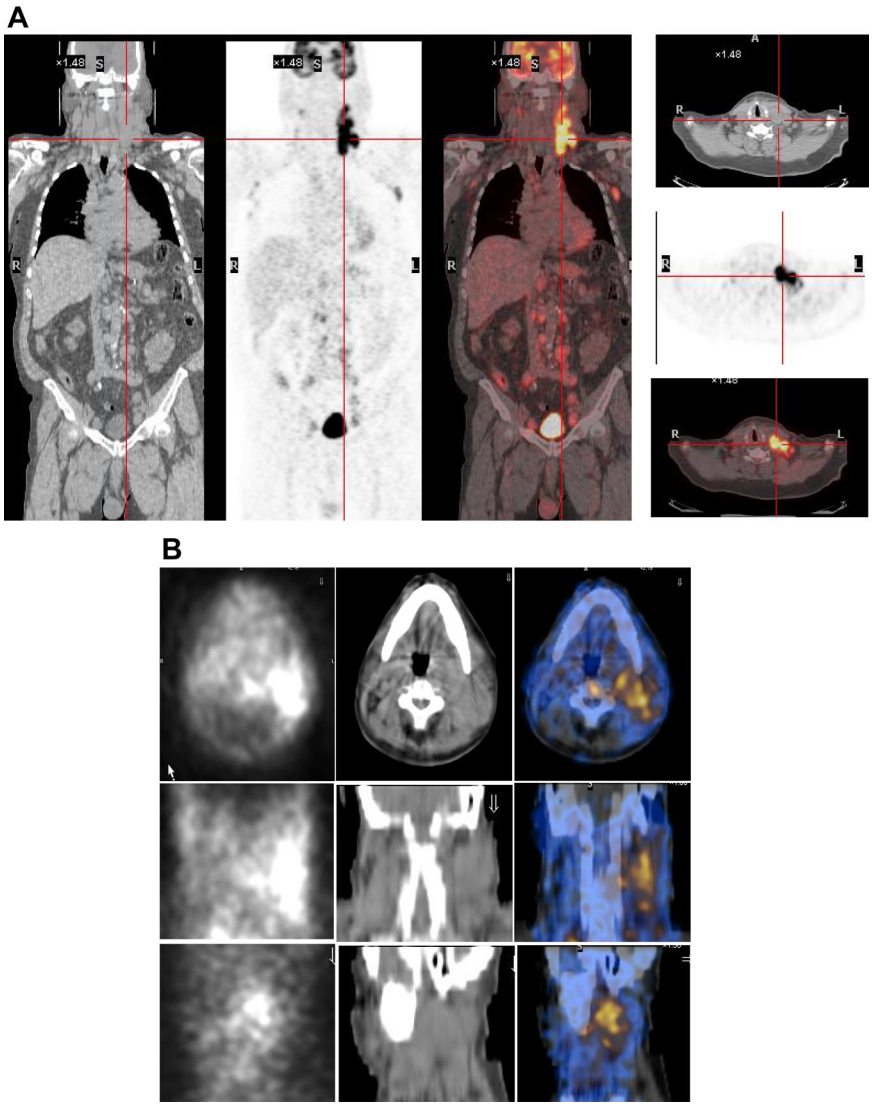

Figure 5. ^{131}I-L19SIP uptake in lymphoma lesions in a patient (NHL1) with SLL NHL. (A) ^{18}F-FDG PET scans demonstrate intense glucose metabolism in multiple enlarged lymph nodes, particularly in the left latero-cervical region. Coronal images are shown in the left panels and transaxial images of the cervical regions are displayed in the right panels. (B) The same patient received an intravenous infusion of 185 MBq and, subsequently, 5.55 GBq ^{131}I-L19SIP. Transaxial, coronal, and sagittal SPECT-CT images of the cervical regions (first, second, and third rows, respectively) were acquired 8 days after the dose of 5.55 GBq. Left column shows scintigraphic images; central column, CT images; and right column, CT-scintigraphy fused images.

leukemia and chronic myeloproliferative diseases, such as CML, polycythemia vera, essential thrombocythemia, or chronic idiopathic fibrosis.

Infiltration of bone marrow by plasmacytoma or lymphoma led to significantly increased ED-B FN expression in comparison with normal bone marrow ($P < .001$).

ED-B FN expression in bone marrow biopsies infiltrated by hematologic malignancies was restricted to small and medium-sized blood vessels consisting of an endothelial layer and a tiny wall of connective tissue. Sinusoids of the bone marrow were also ED-B FN negative in the presence of neoplastic infiltrates.

^{131}I-L19SIP SPECT-CT images and ^{18}F-FDG PET scans

As the radiopharmaceutical ^{131}I-L19SIP contains the very same binding moiety, L19, used for immunohistochemical determination of ED-B FN in lymphoma samples, this radiolabeled agent maintains both high affinity for the target antigen and binding properties typical to other L19 fusion proteins.[35] In the patient with advanced SLL NHL, transaxial, coronal, and sagittal ^{131}I-L19SIP SPECT-CT images demonstrated selective ED-B FN targeting in a palpable, enlarged lymph node conglomerate in the left cervical region, which corresponded to high ^{18}F-FDG uptake on the baseline PET-CT scan (Figure 5). The absorbed dose in the target lesion was estimated at approximately 18 Gy, whereas it was 0.99 Gy and 0.42 Gy in the bone marrow and kidney, respectively. The patient was subsequently treated with a dose of 5.55 GBq ^{131}I-L19SIP. He achieved disease stabilization at 1 month after therapy with the sum of involved lymph node diameters unchanged from baseline (403 vs 417 mm; baseline to 1 month after treatment). However, this patient experienced no clinical benefit from ^{131}I-L19SIP radioimmunotherapy and went off study to receive palliative treatment.

Both HL patients also showed favorable lesion/bone marrow dosimetry estimates after receiving diagnostic ^{131}I-L19SIP, with an absorbed dose of radioactivity to the target lesions—a pulmonary lymphoma lesion (patient HL1) and a left basal pulmonary lesion and a right axillar lymphoma conglomerate (patient HL2)—estimated to be approximately 14 and 22.7 Gy, respectively. The absorbed dose to the red bone marrow was calculated to be 1.3 and 0.85 Gy for HL patients HL1 and HL2, respectively. In HL patient HL1, the SPECT-CT images acquired 12 days after a dose of 5.55 GBq ^{131}I-L19SIP demonstrated selective ED-B FN targeting in multiple parenchymal lung lesions and in enlarged supraclavicular and lumboaortic lymph nodes with all such sites corresponding

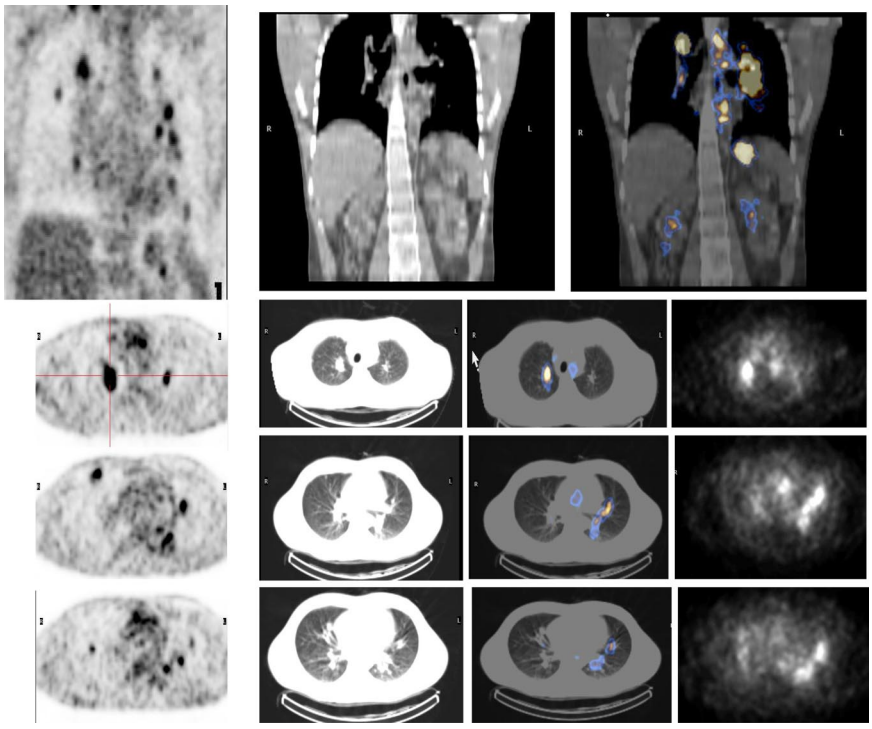

Figure 6. ^{18}F-FDG PET scans and ^{131}I-L19SIP SPECT-CT images from an advanced Hodgkin lymphoma patient (HL1). ^{18}F-FDG PET scans show intense glucose metabolism in multiple enlarged mediastinal lymph nodes, intrapulmonary lesions (leftmost column, first 4 images; intrapulmonary lesion marked), as well as in lumboaortic lymph nodes (leftmost image in lowest row). The same patient received intravenous injections of 185 MBq and, subsequently, 5.55 GBq ^{131}I-L19-SIP. SPECT-CT coronal (top right panel) and transaxial images of the thorax (rows 2-4) as well as the upper abdomen (lowest row) are shown, demonstrating selective uptake of ^{131}I-L19SIP into the ^{18}F-FDG–labeled lymphomatous lesions.

to high ^{18}F-FDG uptake on baseline PET-CT scans (Figure 6). In the second HL patient (HL2), the SPECT-CT images acquired 12 days after a dose of 3.7 GBq ^{131}I-L19SIP demonstrated selective ED-B FN targeting in multiple enlarged axillar and supraclavicular (both sides), paratracheal, subcarinal, pleural, as well as peritoneal and iliacal (both sides) lymph nodes. ED-B FN–expressing lymphoma lesions were also found in the right and left basal lobes of the lung. All ED-B FN–expressing lymphoma lesions corresponded to high ^{18}F-FDG uptake on baseline PET-CT scans (Figure 7). Both HL patients experienced a partial clinical response according to RESCIST criteria at 1 month after therapy with shrinkage of the sum of diameters of the measurable lymphoma lesions of 44% (134 to 75 mm; baseline to 1 month after treatment) and 39% (417 to 256 mm) for patients HL1 and HL2, respectively. This partial response was confirmed at 2 and 3 months after ^{131}I-L19SIP therapy for both HL patients. The 3 lymphoma patients did not experience any acute toxicity during or after ^{131}I-L19SIP therapy. Mild and transient thrombocytopenia was observed in both HL patients, but not in the SLL NHL patient, with a nadir of 22 and 52×10^9 platelets/L for patients HL1 and HL2, respectively, at 6 weeks after ^{131}I-L19SIP injection.

Discussion

The identification of suitable targets for more selective and less toxic therapies for advanced malignant neoplasias is crucial for the success of innovative treatment approaches. Consequently, great emphasis has been put on the identification of unique molecular pathways or specific cellular antigens of malignant cells. Selective treatments interacting with some of these tumor cell–associated targets were found to be highly beneficial, including the monoclonal antibodies rituximab in combination with chemotherapy for B-cell lymphoma,[36] and trastuzumab for Her2/neu overexpressing breast cancer.[37] However, for the majority of advanced solid cancers and for many hematologic malignancies, successful tumor-targeting therapies are still lacking.

Recently, it became clear that stromal structures (eg, blood vessels and extracellular matrix proteins supporting cancer growth and proliferation) are strikingly different from their normal counterparts. As demonstrated by Folkman,[38] neovascularization is crucial for tumor growth beyond 2 mm^3, and was found structurally and functionally altered in comparison with blood vessels of normal mature organs. Vascular shunts, uneven vessel diameters, unusual fenestration with wide interendothelial junctions, discontinuous basement membranes,[39,40] and dysfunctional or lack of pericytes[41,42] are key features of tumor blood vessels that render them leaky. These characteristics may not be specific for tumor blood vessels, since there is evidence of similar changes in blood vessels associated with periodic tissue remodeling,[40,43] chronic inflammatory disease,[28] and severe atherosclerosis.[27] However, targeting anticancer compounds selectively to epitopes that are typically expressed or overexpressed in tumor blood vessels or stroma is attractive for 2 reasons: (1) tumor blood vessel or stromal epitopes are stably expressed, and (2) such epitopes are typically found in all kinds of tumors.

The extra–domain B of fibronectin (ED-B FN) represents such a stromal tumor tissue target.[9] Further validating this concept, the ED-B FN targeting antibody L19 acting as a vehicle for tissue factor or TNFα (tumor necrosis factor α) to the tumor vasculature was found to induce tumor necrosis.[44,45]

ED-B FN expression was found to a variable extent and with different expression patterns by immunohistochemistry on cryostat tissue sections in almost all solid cancers studied thus far.[4] To extend these studies to a reliable sample of hematologic malignancies and to include decalcified bone marrow biopsies, we developed an antigen retrieval technique to stain ED-B FN on paraffin-embedded tissues. This technique led to equivalent immunohistologic staining results on paraffin sections compared with the immunohistologic results on cryostat sections, while preserving

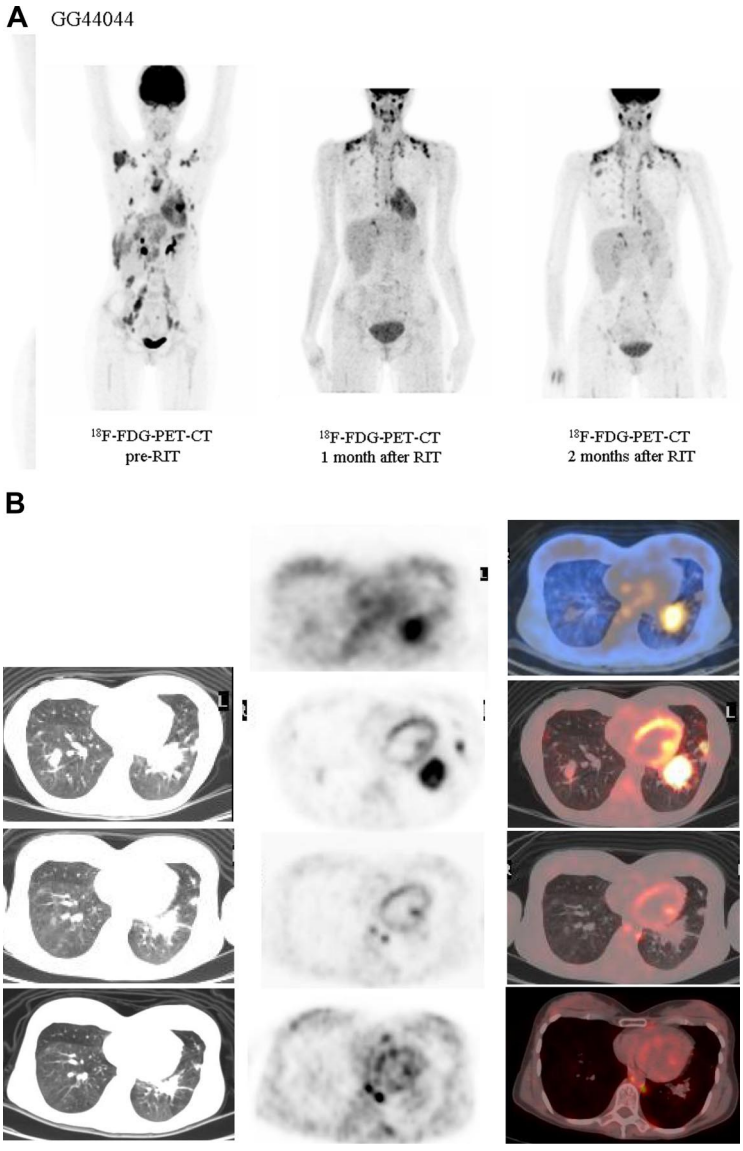

Figure 7. Objective partial remission in another advanced Hodgkin lymphoma patient (HL2) induced by ^{131}I-L19SIP radioimmunotherapy. (A) ^{18}F-FDG PET scans show intense glucose metabolism in multiple enlarged lymph nodes, particularly in right and left axillary and supraclavicular nodes, in paratracheal, subcarinal, peritoneal, and iliacal nodes as well as in lymphoma lesions located in the basal lobes of both lungs (leftmost image). One (center) and 2 (rightmost image) months after application of therapeutic ^{131}I-L19SIP (3.7 GBq), the number and size of active lymphoma lesions decreased substantially. (B) ^{18}F-FDG PET scans and ^{131}I-L19SIP SPECT-CT images from the same patient. Transaxial SPECT-CT images (top row) show selective ^{131}I-L19SIP uptake to a pulmonary lymphoma lesion still detectable 12 days after injecting a therapeutic dose (3.7 GBq). Transaxial ^{18}F-FDG PET scans captured prior to (second row), 1 month after (third row) and 2 months after (bottommost row) application of therapeutic ^{131}I-L19SIP show a significant shrinkage in size and a complete disappearance of metabolic activity in the initially large pulmonary lymphoma lesion, indicative of lymphoma response to ^{131}I-L19SIP radioimmunotherapy.

tissue histology. The loss of ED-B FN staining in tissue sections after addition of soluble recombinant ED-B FN to the anti–ED-B FN reagents demonstrated the specificity of the immunohistochemical procedure. Thus, we are able to present the first systematic report of ED-B FN expression on normal lymphoid and hematopoietic tissue and in a large series of lymphoid and hematologic malignancies, including decalcified bone marrow biopsies.

We found expression of ED-B FN in almost all examined lymphoma samples, irrespective of their histopathologic classification. ED-B FN–positive vessels were significantly more tightly packed in lymph nodes with lymphoma infiltration than in the tumor-free lymph nodes draining carcinomas. Low-grade non-Hodgkin lymphomas contained fewer ED-B FN–positive vessels than high-grade lymphoma, indicating that neoangenesis is correlated with the proliferation rate of tumor cells. The same holds true for bone marrow samples infiltrated by lymphoma or leukemia, revealing high perivascular ED-B FN expression, whereas normal bone marrow biopsies are almost ED-B FN negative. However, the strong ED-B FN expression in lymph nodes with severe inflammation and in hyperplastic tonsils causing angina, as a consequence of the fast expansion of lymphoid tissue in response to viral or bacterial infection, confirms that ED-B FN expression is a general feature of rapidly proliferating and remodeling tissues, independent from the cause inducing these processes.

We could not detect cytoplasmatic ED-B FN expression in megakaryocytes. This finding is only partially consistent with the results of Vogel et al[46] who found ED-B FN in megakaryocytes by immunocytologic analyses of bone marrow smears but could not confirm these findings by flow cytometric analysis or reverse-transcription polymerase chain reaction (PCR).

Wagner et al[47] and Blum et al[48] found weak ED-B FN expression on the surface of CD3- and IL-2–stimulated T cells by flow cytometry. Since immunohistochemistry is less sensitive than flow cytometry, our results may be interpreted as a consequence of a very low ED-B FN expression level in stimulated T cells.

To confirm perivascular ED-B FN expression, we performed immunofluorescence double stainings of ED-B FN–positive and CD34$^+$ endothelia. These investigations indicate that ED-B FN in hematologic malignancies is almost always associated with the wall of blood vessels and the perivascular connective tissue. In all specimens of lymphoid and hematopoietic tissues, there was only a small amount of ED-B FN displaying an unequivocally extravascular localization. From the perspective of designing antibody-based

tumor targeting therapies, ED-B FN in newly formed blood vessels is of particular relevance compared with stromal ED-B FN, since it is easily accessible from the bloodstream due to the frequent fenestrations and leakiness of tumor blood vessels.[40]

These considerations were confirmed by our exploratory proof-of-mechanism investigations, demonstrating the accessibility of lymphoma-associated ED-B FN expression via the bloodstream as well as respective ED-B antibody binding properties in vivo. ^{131}I-L19SIP was intravenously injected into patients suffering from relapsed advanced SLL-NHL and HL (n = 2). Subsequently performed scintigraphic in vivo images demonstrated selective expression and accessibility of lymphoma-associated ED-B FN in these 3 patients, confirming and extending previously published immunoscintigraphic studies with radioisotope-labeled ED-B antibodies in patients with solid cancer. In a small study of 5 patients with malignant brain tumors, planar and SPECT-CT imaging using the ^{99m}Tc-labeled ED-B monoclonal antibody BC-1 disclosed the brain tumors in all cases.[49] In another study with 20 patients suffering from advanced lung, colorectal, or brain cancers, selective localization of ED-B binding ^{123}I-L19(scFv)$_2$ to tumor lesions was demonstrated.[50] In our lymphoma patients, the uptake of ^{131}I-L19SIP to lymphoma lesions was not only selective and long-lasting (up to 12 days after injection), but also surprisingly high with an absorbed dose to the target lesion of approximately 14 to 22.7 Gy, sparing radiosensitive organs such as red bone marrow and the kidneys. Furthermore, the 2 HL patients experienced a sustained partial remission according to response evaluation criteria in solid tumors (RECIST), which was associated with clinical benefit, lasting for at least 2 and 3 months. In contrast, the SLL-NHL patient had only short disease stabilization and did not benefit from treatment.

In conclusion, developing an antigen-retrieval method for immunohistochemistry on paraffin sections, we were able to demonstrate ED-B FN depositions in the extracellular matrix on newly formed blood vessels in hematologic malignancies. The application of the highly ED-B FN–specific radiolabeled antibody ^{131}I-L19SIP in 3 lymphoma patients confirms the in vivo accessibility of this target in humans. The induction of a partial remission in 2 relapsed HL patients shows that therapeutic doses of radioactivity can be selectively delivered by ^{131}I-L19SIP to Hodgkin lymphoma lesions. Together, these data suggest that the molecular composition of newly formed vessel walls in hematologic malignancies (1) is equivalent to those of solid cancers, and (2) is accessible for intravenous antibody treatments. Thus, these data qualify ED-B FN as a very promising target for L19-based cancer therapies (eg, ^{131}I-L19SIP) in lymphoma patients. For solid cancer patients (renal cell and pancreatic cancer), the clinical evaluation of similar approaches is ongoing (eg, L19IL2).[51]

Acknowledgments

The authors thank Conny Cieluch, Martina Sollini, Claudio Traino, and Heidrun Protz for their technical assistance in performing the study and Ava Coe for her editorial help in the preparation of this paper.

This study was partially funded by Bayer Schering Pharma, Berlin, Germany.

Authorship

Contribution: S.S. analyzed the tissue sections for ED-B expression; P.A.E. performed the clinical research on the lymphoma patients; A.M. contributed vital new reagents and analytic tools and analysis; P.A.E., M.P., G.M., C.G., and G.P. cared for the patients, designed the clinical research, and collected the ^{131}I-L19SIP SPECT-CT images; L.G., B.H., L.Z., and D.N. analyzed the data and reviewed the paper; and H.D. and H.D.M. designed the research, supervised the workflow, analyzed and interpreted the results, and wrote the paper.

Conflict-of-interest disclosure: H.D.M. owns few regular stocks since February 2008. H.D. received a research grant from Bayer-Schering Pharma, Berlin, Germany. The remaining authors declare no competing financial interests.

Correspondence: Hans D. Menssen, Bayer HealthCare Pharmaceuticals, PO Box 1000, Montville, NJ 07045-1000; e-mail: hansdietrich.menssen@bayer.com.

References

1. Skipper HE. Laboratory models: the historical perspective. Cancer Treat Rep. 1986;70:3-7.
2. Taskin AL, Legrand O, Raffoux E, et al. High efficacy and safety profile of Mylotarg as induction therapy in patients with relapsed acute myeloblastic leukemia: a prospective study of the alfa group. Leukemia. 2007;21:66-71.
3. Osenga KL, Hank JA, Albertini MR, et al. A phase I clinical trial of the hu14.18-IL2 (EMD 273063) as a treatment for children with refractory or recurrent neuroblastoma and melanoma: a study of the Children's Oncology Group. Clin Cancer Res. 2006;12:1750-1759.
4. Menrad A, Menssen HD. ED-B fibronectin as a target for antibody-based cancer treatments. Expert Opin Ther Targets. 2005;9:1-10.
5. Hynes RO. Molecular biology of fibronectin. Annu Rev Cell Biol. 1985;1:67-90.
6. Ruoslahti E. Fibronectin and its receptors. Annu Rev Biochem. 1988;57:375-413.
7. Petersen TE, Thogersen HC, Skorstengaard K, et al. Partial primary structure of bovine plasma fibronectin: Three types of internal homology. Proc Natl Acad Sci U S A. 1983;80:137-141.
8. Hynes RO. Fibronectins. New York, NY: Springer-Verlag; 1990.
9. Zardi L, Carnemolla B, Siri A, et al. Transformed human cells produce a new fibronectin isoform by alternative splicing of a previously unobserved exon. EMBO J. 1987;6:2337-2342.
10. Carnemolla B, Balza E, Siri A, et al. A tumor-associated fibronectin isoform generated by alternative splicing of messenger RNA precursors. J Cell Biol. 1989;108:1139-1148.
11. Ffrench-Constant C, Hynes RO. Alternative splicing of fibronectin is temporally and spatially regulated in chicken embryo. Development. 1989;106:317-329.
12. Midulla M, Verma R, Pignatelli M, Ritter MA, Courtenay-Luck AJ. Source of oncofetal ED-B-containing fibronectin: implications of production by both tumor and endothelial cells. Clin Cancer Res. 2000;8:540-548.
13. Berndt A, Borsi L, Xinmel, et al. Evidence of ED-B+ fibronectin synthesis in human tissues by non-radioactive RNA in situ hybridization: investigation on carcinoma (oral squamous cell and breast cancer), chronic inflammation (rheumatoid synovitis) and fibromatosis (Morbus Dupytren). Histochem Cell Biol. 1998;109:249-255.
14. Kosmehl H, Berndt A, Strassburger S, et al. Distribution of lamin and fibronectin isoforms in oral mucosa and oral squamous cell carcinoma. Br J Cancer. 1999;81:1071-1079.
15. Pujuguet P, Hammann A, Mouttet M, et al. Expression of fibronectin ED-A+ and ED-B+ isoforms by human and experimental colorectal cancer: contribution of cancer cells and tumor-associated myofibroblasts. Am J Pathol. 1996;148:579-592.
16. Zang DW, Burton-Wurster N, Lust G. Antibody specificity for extra domain B of fibronectin demonstrates elevated levels of both extra domain B(+) and B(-) fibronectin in osteoarthritic canine cartilage. Matrix Bio. 1994;14:623-633.
17. Peters JH, Trevithick JE, Johnson P, Haynes RO. Expression of the alternatively spliced EIIIB segment of fibronectin. Cell Adhes Commun. 1995;3:67-89.
18. Carnemolla B, Neri D, Castellani P, et al. Phage antibodies with pan-species recognition of the oncofetal angiogenesis marker fibronectin ED-B domain. Int J Cancer. 1996;68:397-405.
19. Ffrench-Constant C, Van de Water L, Dvorak HF, Hynes RO. Reappearance of an embryonic pattern of fibronectin splicing during wound healing in the adult rat. J Cell Biol. 1989;109:903-914.

20. Fukuda T, Yoshida N, Kataoka Y, et al. Mice lacking the EDB segment of fibronectin develop normally but exhibit reduced cell growth and fibronectin matrix assembly in vitro. Cancer Res. 2002;62:5603-5610.
21. Astrof S, Crowley D, George EL, et al. Direct test of potential roles of EIIIA and EIIIB alternatively spliced segments of fibronectin in physiological and tumor angiogenesis. Mol Cell Biol. 2004;24:8662-8670.
22. Astrof S, Crowley D, Hynes RO. Multiple cardiovascular defects caused by the absence of alternatively spliced segments of fibronectin. Dev Biol. 2007;311:11-24.
23. Castellani P, Viale G, Dorcaratto A, et al. The fibronectin isoform containing the ED-B oncofetal domain: a marker of angiogenesis. Int J Cancer. 1994;59:612-618.
24. Castellani P, Borsi L, Carnemolla B, et al. Differentation between high and low grade astrocytoma using a human recombinant antibody to the ED-B domain of fibronectin. Am J Pathol. 2002;161:1695-1700.
25. Birchler M, Viti F, Zardi L, et al. Selective targeting and photocoagulation of ocular angiogenesis mediated by a phage derived human antibody fragment. Nat Biotechnol. 1999;17:984-988.
26. Nicolò M, Biro A, Cardillo-Piccolino F, et al. Expression of extradomain-B-containing fibronectin in subretinal choriodal neovascular membranes. Am J Ophthalmol. 2003;135:7-13.
27. Matter CM, Schuler PK, Alessi P, et al. Molecular imaging of atherosclerotic plaques using a human antibody against the extra-domain B of fibronectin. Cir Res. 2004;95:1223-1233.
28. Kriegsmann J, Berndt A, Hansen T, et al. Expression of fibronectin splice variants and oncofetal glycosylated fibronectin in the synovial membranes of patients with rheumatoid arthritis and osteoarthritis. Rheumatol Int. 2004;24:25-33.
29. Jaffe ES, Harris NL, Stein H, Vardiman JM, eds. World Health Organization Classification of Tumours, Pathology & Genetics: Tumours of Haematopoietic and Lymphoid Tissues. Lyon, France: IARC Press; 2001.
30. Carnemolla B, Borsi L, Balza E, et al. Enhancement of the antitumor properties of interleukin-2 by its targeted delivery to the tumor blood vessel extracellular matrix. Blood. 2002;99:1659-1665.
31. Cordell J, Falini B, Erber ON, et al. Immunoenzymatic labeling of monoclonal antibodies using immune complexes of alkaline phosphatase and monoclonal anti-alkaline phosphatase (APAAP complexes). J Histochem Cytochem. 1984;32:219-229.
32. Pini A, Viti F, Santucci A, et al. Design and use of a phage display library: human antibodies with subnanomolar affinity against a marker of angiogenesis eluted from a two-dimensional gel. J Biol Chem. 1998;273:21769-21776.
33. Viti F, Tarli L, Giovannoni L, et al. Increased binding affinity and valence of recombinant antibody fragments lead to improved targeting of tumoral angiogenesis. Cancer Res. 1999;59:347-352.
34. Bombardieri E, Coliva A, Chiesa C, et al. Phase I study with antifibronectin I-131-L19SIP: First dosimetric and therapeutic results. J Nucl Med. 2007;48(suppl 2):398. Abstract 1681.
35. Ebbinghaus C, Scheuermann J, Neri D, Elia G. Diagnostic and therapeutic applications of recombinant antibodies: targeting the extradomain B of fibronectin, a marker of tumor angiogenesis. Curr Pharm Des. 2004;10:1537-1549.
36. Coiffier B. Standard treatment of advanced-stage diffuse large B-cell lymophoma. Semin Hematol. 2006;43:213-220.
37. Smith I, Procter M, Gelber RD, et al. 2-year follow-up of trastuzumab after adjuvant chemotherapy in HER2-positive breast cancer: a randomized controlled trial. Lancet. 2007;368:29-36.
38. Folkman J. The role of angiogenesis in tumor growth. Sem Cancer Biol. 1992;3:65-71.
39. Dewhirst MW, Tso CY, Oliver R, et al. Morphologic and hemodynamic comparison of tumor and healing normal tissue microvasculature. Int J Radiat Oncol Biol Phys. 1989;17:91-99.
40. Cohen MM Jr. Vascular update: morphogenesis, tumors, malformations, and molecular dimensions. Am J Medical Genetics A. 2007;140A:2013-2038.
41. Eberhard A, Kahlert S, Goede V, et al. Heterogeneiity of angiogenesis and blood vessel maturation in human tumors: implication for angiogenetic tumor therapies. Cancer Res. 2000;60:1388-1393.
42. Morikawa S, Baluk P, Kaidoh T, et al. Abnormalities in pericytes on blood vessels and endothelial sprouts in tumors. Am J Pathol. 2002;160:985-1000.
43. De Candia LM, Rogers RJ. Characterization of the expression of the alternative splicing of the ED-A, ED-B, and V-regions of fibronectin mRNA in bovine ovarian follicles and corpora lutea. Repr Fert Dev. 1999;11:367-377.
44. Huang X, Molema G, King S, et al. Tumor infarction in mice by antibody-directed targeting of tissue factor to tumor vasculature. Science. 1997;275:547-550.
45. Borsi L, Balza E, Carnemolla B, et al. Selective targeted delivery of TNF alpha to tumour blood vessels. Blood. 2003;102:4384-4392.
46. Vogel W, Berndt A, Mueller A, et al. Differential in vivo and in vitro expression of ED-B+ fibronectin in adult human hematopoiesis. Int J Molecul Med. 2003;12:831-837.
47. Wagner C, Bürger A, Radsak M, et al. Fibronectin synthesis by activated T lymphocytes: up-regulation of a surface-associated isoform with signaling function. Immunology. 2000;99:532-539.
48. Blum S, Hug F, Haenschb GM, Wagner C. Fibronectin on activated T lymphocytes is bound to gangliosides and is present in detergent insoluble microdomains. Immunol Cell Biol. 2005;83:167-174.
49. Mariani G, Lasku A, Pau A, et al. A pilot immunoscintigraphic and pharmacokinetic study with the Technetium-99m-labeled monoclonal antibody BC-1 directed against oncofetal fibronectin in patients with brain tumors. Cancer. 1997;80:2484-2489.
50. Santimaria M, Moscatelli G, Viale GL, et al. Immunoscintigraphic detection of the ED-B domain of fibronectin, a marker of angiogenesis, in patients with cancer. Clin Cancer Res. 2003;9:571-579.
51. Curigliano G, Spitalieri G, DePas T, et al. A dose-finding pharmacokinetic study of the tumor-targeting human L19IL2 monoclonal antibody-cytokine fusion protein in patients with advanced solid tumors. J Clin Oncol. ASCO Annual Meeting Proceedings. 2007; Abstract 3057.